Photon-Counting Lidar for Aerosol Detection and 3-D Imaging

Citation: Marino, Richard M. et al. "Photon-counting lidar for aerosol detection and 3D imaging." Laser Radar Technology and Applications XIV. Ed. Monte D. Turner & Gary W. Kamerman. Orlando, FL, USA: SPIE, 2009. 73230H-10. © 2009 SPIE

As Published: http://dx.doi.org/10.1117/12.819179

Publisher: Society of Photo-optical Instrumentation Engineers

Persistent URL: http://hdl.handle.net/1721.1/52655

Version: Final published version: final published article, as it appeared in a journal, conference proceedings, or other formally published context

Photon-Counting Lidar for Aerosol Detection and 3-D Imaging[§]

Richard M. Marino[1], Jonathan Richardson[2], Robert Garnier,
David Ireland, Laura Bickmeier, Christina Siracusa, Patrick Quinn
Massachusetts Institute of Technology, Lincoln Laboratory,
244 Wood Street, Lexington, MA USA 02420

ABSTRACT

Laser-based remote sensing is undergoing a remarkable advance due to novel technologies developed at MIT Lincoln Laboratory. We have conducted recent experiments that have demonstrated the utility of detecting and imaging low-density aerosol clouds. The Mobile Active Imaging LIDAR (MAIL) system uses a Lincoln Laboratory-developed microchip laser to transmit short pulses at 14-16 kHz Pulse Repetition Frequency (PRF), and a Lincoln Laboratory-developed 32x32 Geiger-mode Avalanche-Photodiode Detector (GmAPD) array for single-photon counting and ranging. The microchip laser is a frequency-doubled passively Q-Switched Nd:YAG laser providing an average transmitted power of less than 64 milli-Watts. When the avalanche photo-diodes are operated in the Geiger-mode, they are reverse-biased above the breakdown voltage for a time that corresponds to the effective range-gate or range-window of interest. The time-of-flight, and therefore range, is determined from the measured laser transmit time and the digital time value from each pixel. The optical intensity of the received pulse is not measured because the GmAPD is saturated by the electron avalanche. Instead, the reflectivity of the scene, or relative density of aerosols in this case, is determined from the temporally and/or spatially analyzed detection statistics.

There are several advantages to sensor architectures that use direct detection and arrays of photon-counting detectors. Perhaps the most significant advantage is a reduced requirement for power-aperture product of more than an order of magnitude. In this paper, we describe the LIDAR sensor system used in MAIL, and our experimental results showing system sensitivity, and temporal and spatially resolved releases of aerosol clouds within a controlled chamber.

Keywords: Lidar, ladar, laser radar, 3D imaging, aerosol detection, photon-counting, Geiger-mode, avalanche photodiode detector array

1. INTRODUCTION

Several mission areas require the application of remote sensors to detect and locate the release of aerosol agents. Furthermore, the capacity to detect and track aerosol clouds with low-latency is required to enable responsive defenses. Recent demonstrations of active ladar or lidar imaging with laser illumination and photon-counting receivers have proven that the sensor system can be compact and robust [1-7]. MIT Lincoln Laboratory developed the Mobile Active Imaging Ladar (MAIL) as a transportable testbed to help investigate the performance of a 3D imaging laser radar sensor system with photon-counting sensitivity. Figure 1 shows the MAIL van and sensor system, and the ladar sensor parameters are listed in Table 1. The goals of the test were to: 1) determine the detection sensitivity limit for this photon-counting ladar sensor, and 2) measure the spatial and temporal distribution of point releases of aerosol samples within a controlled chamber.

[§] *This work is sponsored by the United States Army under Air Force Contract FA8721-05-C-0002. Opinions, interpretations, conclusions and recommendations are those of the author and are not necessarily endorsed by the United States Government.*
[1] marino@ll.mit.edu; phone 1 781 981-4011; fax 1 781 981-5069
[2] richardson@ll.mit.edu

Laser Radar Technology and Applications XIV, edited by Monte D. Turner, Gary W. Kamerman,
Proc. of SPIE Vol. 7323, 73230H · © 2009 SPIE · CCC code: 0277-786X/09/$18 · doi: 10.1117/12.819179

Figure 1. The Mobile Active Imaging Ladar sensor system (MAIL van)

Although the MAIL system was developed and proven to image hard macroscopic targets, such as buildings and ground vehicles, we wanted to investigate the sensitivity and utility of photon-counting ladar for standoff detecting and imaging thin or low-density aerosol clouds. The high-sensitivity (using a Geiger-mode avalanche photodiode detector [GmAPD] array) and relatively high pulse repetition and 3-D imaging frequency (PRF ~ 15-16 kHz) of the sensor was crucial in successfully demonstrating spatially and temporally resolved imagery of aerosol releases within a controlled chamber (The Vortex Chamber at the US Army Edgewood Chemical Biological Center, Edgewood, MD [http://www.ecbc.army.mil/ps/svcs_env_field_test_vortex.html]).

2. THE TEST SETUP FOR AEROSOL IMAGING

The Vortex Chamber was used to distribute a known quantity of dry aerosols (typically, a small quantity of Arizona Road Dust (AZRD) comprised of clay particles of known sizes). AZRD is a "standard" non-hazardous material that was ordered with specified particle sizes. Two size ranges were used in our tests: A) particles of size less than or equal to 5-micrometers [AZRD_0-5], B) particles of size greater than 5-micrometers but less than or equal to 10-micrometers [AZRD_5-10]. HEPA filters are used to remove ambient and/or released particulates from a portion of the air circulating within the chamber. One or two point detectors estimate particle density and size distribution every 5 seconds. The typical data acquisition sequence during a release test was as follows:

1) The Vortex Chamber is operated for roughly 10 minutes to remove ambient aerosols. Under operating conditions of these tests, the HEPA filters reduce the aerosol density within the chamber at a rate of roughly 10 dB every 10 minutes (until the average ambient density is reduced to about 1 particle per cc).

2) A sample of AZRD is released into the circulating air from a point dispenser after the ambient aerosol density is reduced to less than 1 particle per cc. The sample masses for our tests ranged from 16-mg to 1-g.

3) Ladar data was recorded before during and after the release of a given sample. The laser and FPA were operated at 12.5 to 14.5 kHz pulse and framing rate.

4) A calibration plate (Spectralon 2% diffuse reflectivity) was located just beyond the Vortex Chamber and at a range of about 83-m from the ladar sensor.

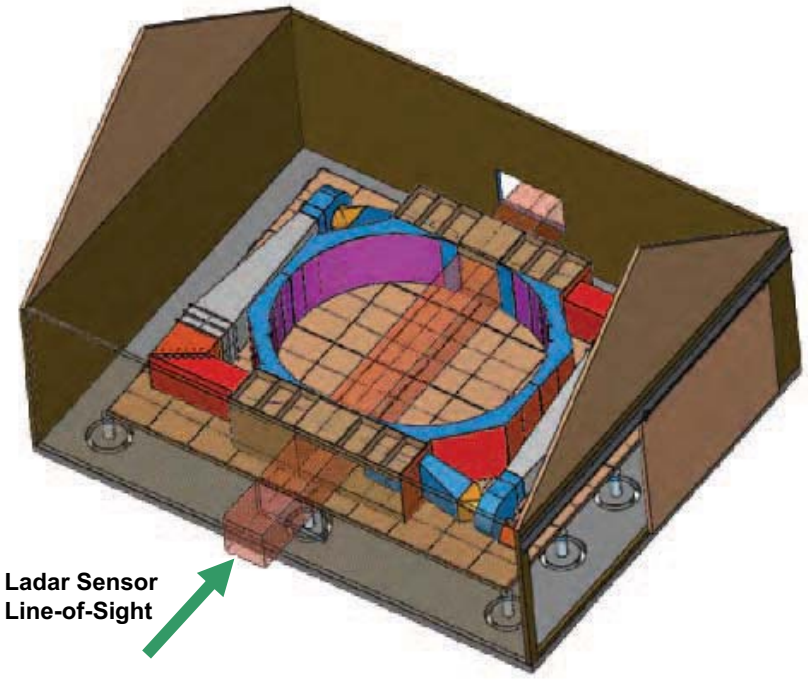

Figure 2. The ECBC Windowless Vortex Chamber with volume of 67 cubic meters and 6.1 m path length

Table 1. MAIL Ladar Sensor System Parameters

Parameter	Value	Comment
Telescope magnification	750	Fixed
Field of Regard	10.8 deg	Using integrated scanner (two rotating Risley prisms)
Laser Wavelength	532 nm	
Laser far field beam pattern	32 x 32 spot array	Aligned with detector IFOV array
Laser pulse width	300 ps	Full width half max
Laser Pulse and Raw Imaging Rate	16,000 per s (max)	Imaging over 32x32 array only
Outgoing Laser Pulse Energy	4 μJ (max)	Can be attenuated
Receive aperture diameter	7.5 cm	
Effective focal length	300 mm	
Focal ratio	*f*/4.0	
Number of pixels in FPA	32 x 32	
Projected 100 μm pixel pitch	333 μrad	
Instantaneous Cross-Range Sample	5 cm at 150 m range	< 7.5 cm goal
FPA FOV (32 x 32)	10.1 mrad x 10.1 mrad	
Range Resolution	40 cm	> 7.5 cm goal
FPA Range Sampling Rate	2 GHz effective	500 GHz plus two vernier bits
Instantaneous Field of Regard	10.1 mrad by 10.1 mrad	1.51 m square at 150 m range (32x32 array)

Data were recorded for a total of ten releases. An Aerodynamic Particle Sizer (APS) Spectrometer Model 3321 from TSI (http://tsiinc.eu/documents/3321.pdf) was used to monitor particle density and size distribution, as measured at one location within the Vortex Chamber. Figure 3 shows a plot of the data recorded by the APS for these ten releases. The plot shows a floor or minimum observed concentration of about 0.6 particles per cc. This minimum may be due to the noise limit of the APS and/or the limit to which the Vortex Chamber could remove ambient aerosols (possibly due to particle size limitations of he HEPA filters and/or infiltration of exo-chamber ambient aerosols through the open ports of the Vortex Chamber).

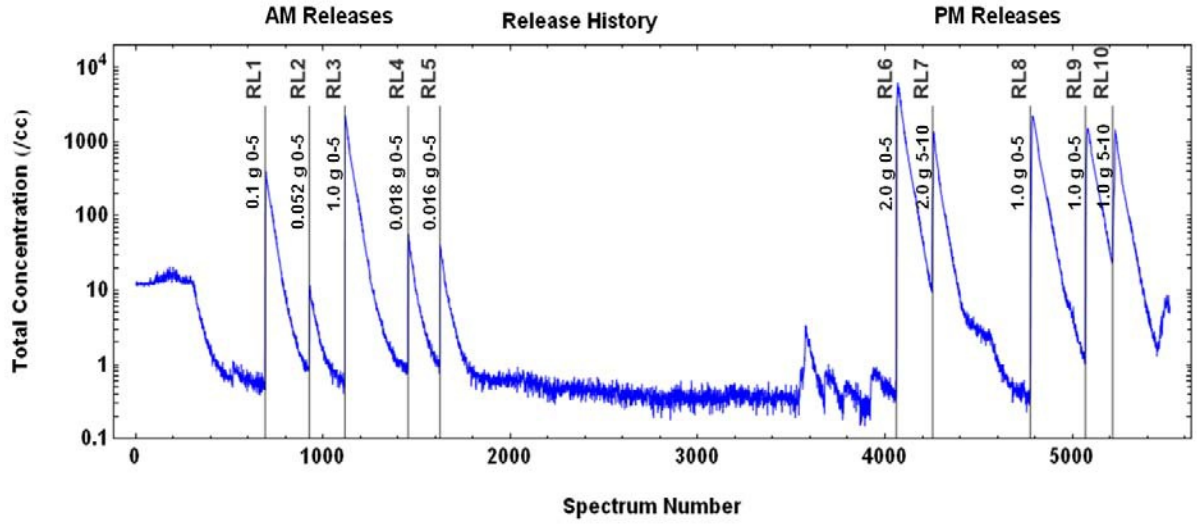

Figure 3. The history of APS-measured particle concentration during the test campaign.

Batches of dry AZRD were acquired beforehand in specified ranges of particle sizes. For these tests, the range AZRD particle sizes were selected from two batches: A) 0-5 microns diameter, and B) 5-10 micron diameter. From these batches, a small sample was selected and its mass measured before insertion into the injector subsystem. Table 2 lists the sample sizes and particle size ranges used in the ladar tests performed. Figure 4 shows a photograph of a sample of AZRD of particle size diameters within the range of 0-5 microns on a white plastic spoon. The measurement of the mass of this sample is shown to be 0.016 grams.

Table 2. Samples of Arizona Road Dust (AZRD) Used

Test Sequence	Range of Particle Sizes	Mass of Sample
1, 2	0-5 microns	1.0 gram
3, 4	0-5 microns	0.1 gram
5	0-5 microns	0.053 gram
6	0-5 microns	0.018 gram
7	0-5 microns	0.016 gram
8	0-5 microns	2.0 gram
9	5-10 microns	2.0 gram
10	0-5 microns	1.0 gram
11	5-10 microns	1.0 gram

Figure 4: Sixteen milligrams of AZRD 0-5 microns.

Figure 5 shows a photograph of the ladar sensor head in the foreground with the Vortex Chamber building in the far ground or out-range. The building wall closest to the sensor was at a range of approximately 68-meters. Although the ladar sensor head includes two counter-rotating Risley prisms to direct and scan the co-aligned transmit and receive optical axes, these were not used for scanning during these aerosol tests. Instead, the range from the sensor to the chamber was selected to match the ladar's static filed-of-view (FOV) and the size of the chamber far-side window. That is, the ladar's 32x32 laser spot pattern was aligned to pass through the open building door and through the Vortex Chamber

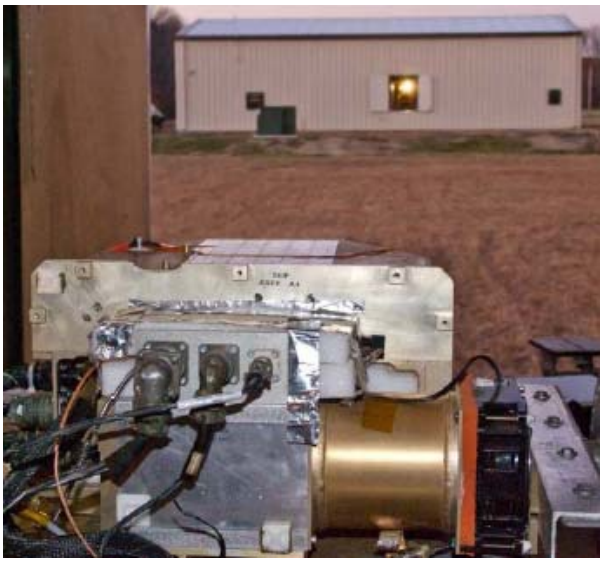

Figure 5: A photograph of the ladar sensor head in the foreground with the Vortex Chamber building in the far ground or out-range.

Figure 6 shows a photograph taken from within the building, on the far side of the Vortex Chamber itself, and with the camera pointing in the general direction of the ladar sensor. This image shows the green (532-nm wavelength) laser light forward-scattered from some distributed aerosols within the chamber, and the more intense scatter near the injection nozzle during a release of additional particulates.

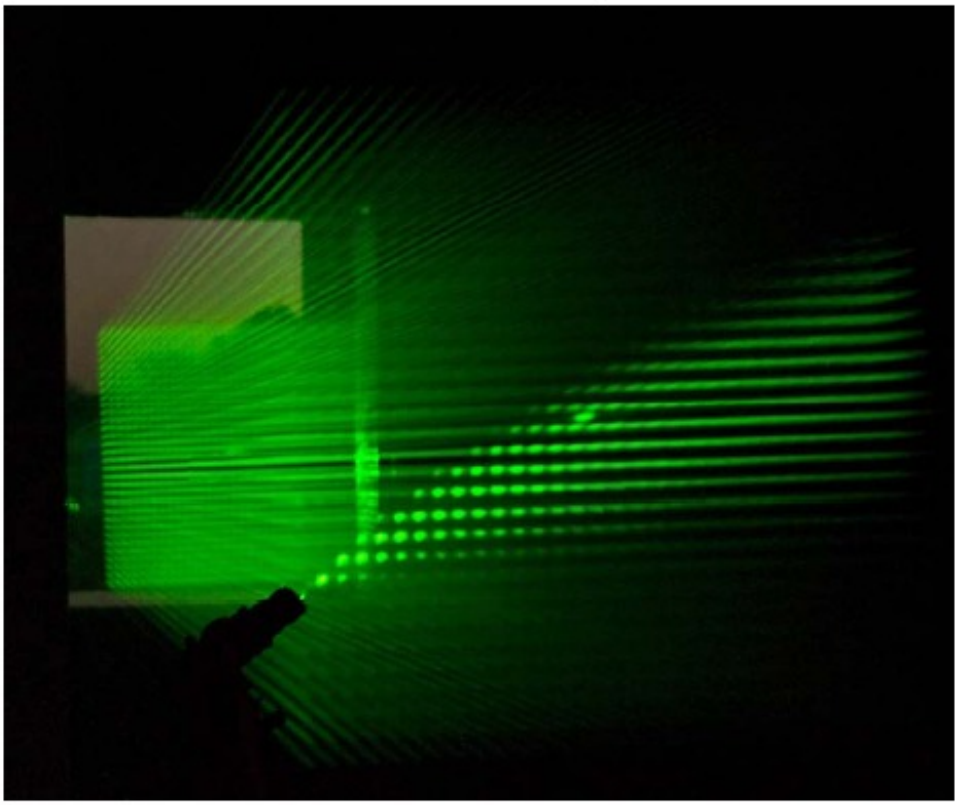

Figure 6: A photograph shows the green (532-nm wavelength) laser light forward-scattered from the aerosols within the chamber, and the relatively greater scatter near the injection nozzle during a release.

3. LADAR SENSOR DATA PROCESSING

Background data were recorded before each release. The raw ladar data were processed by first subtracting average background counts and then integrating spatially (by angle) and/or in range and/or in time to render the spatial and/or temporal distributions of the released aerosols. Of course, the signal-to-noise ratio (SNR) is improved with increasing integration of these spatial-temporal dimensions. Examples of the recorded data set are displayed here in a variety of integration formats.

Figure 7 shows a temporal series of range-resolved intensity histograms of the aerosol-backscatter signal. The relatively large bump in figure 7a corresponds to the spatially resolved "puff" of aerosols. The distribution of aerosols begins from one location (the nozzle) and slowly spreads out to a nearly uniform distribution after several cycles of the air within the chamber (as shown in figure 7c). These data were the first measurement of the temporal-spatial distribution of aerosols from a point release, and that the Vortex Chamber does indeed achieve the design goal of uniform aerosol density.

The density of aerosols slowly decreases as a portion of the aerosol is entrained with the outer horizontal circulating air curtain and are removed by the HEPA filters.. The rate at which the HEPA filers removed the mixed aerosols, as measured by the single APS particle counter, is estimated from figure 3 to be roughly 10 dB every 10 minutes.

A second method to process the background-subtracted ladar data is to reveal the 2-D spatial distribution of aerosol density versus time. Figure 8 shows the (32 pixel by 32 pixel) angle-angle-resolved intensity image for a range

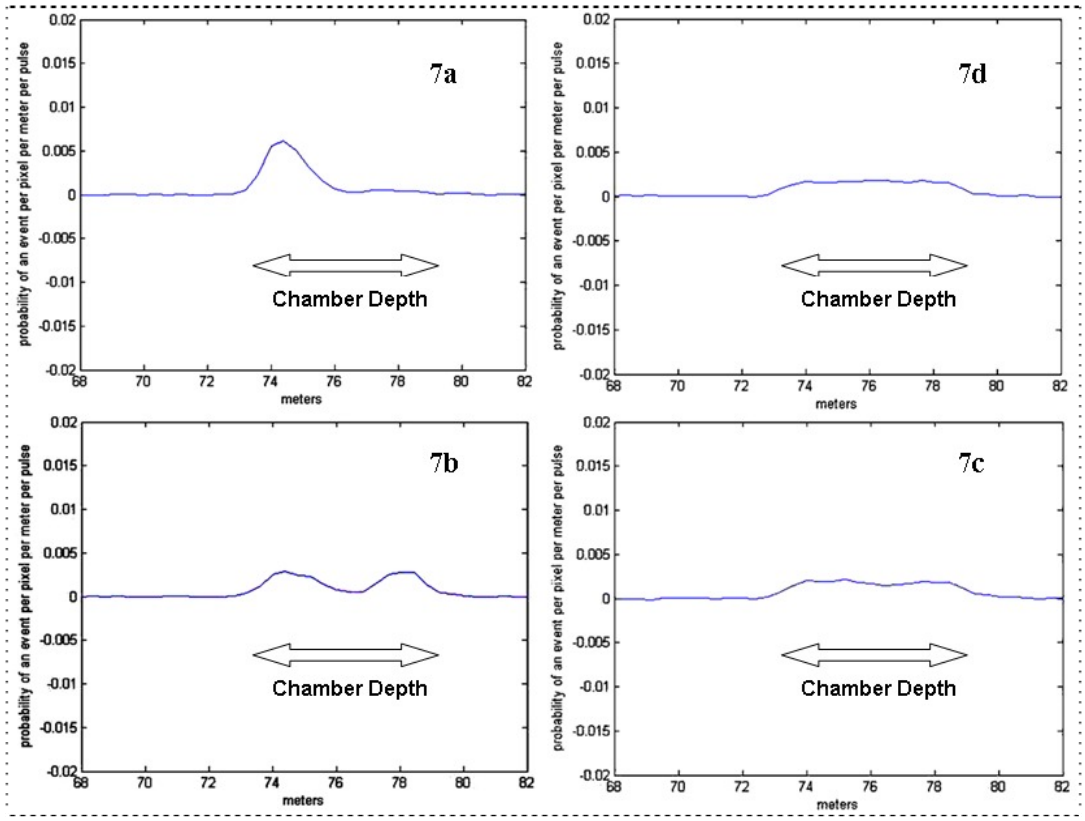

Figure 7: A temporal series of range-resolved intensity histograms of the aerosol-backscatter signal, in normalized units of ***probability of detection per pixel per meter per laser pulse***. *Video 1*
http://dx.doi.org/10.1117/12.819179.1

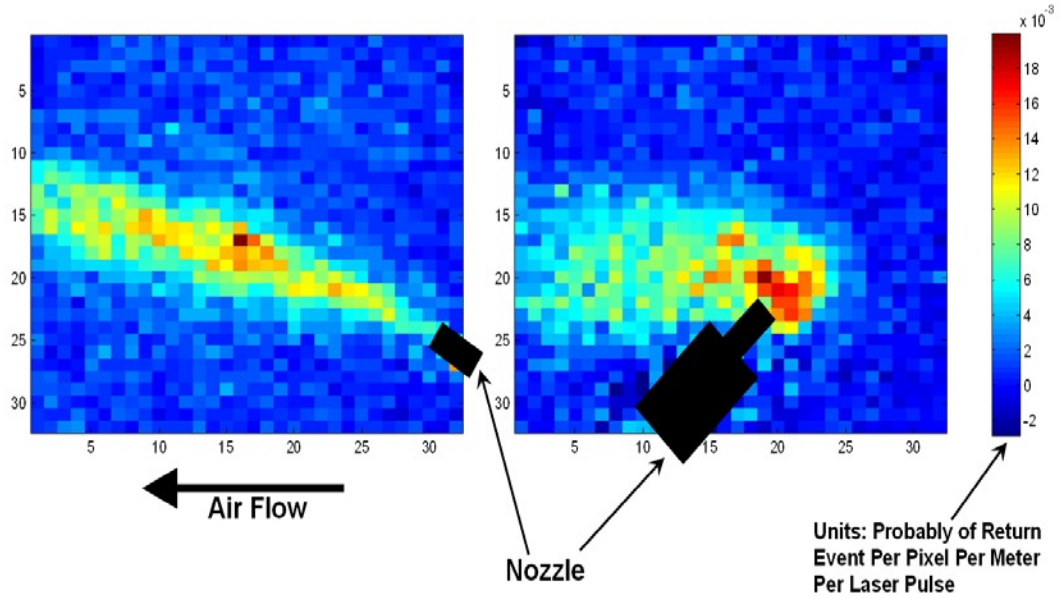

Figure 8: Angle-angle-resolved intensity images from a range-gate that includes the insertion nozzle; a) with the nozzle pointed upstream of the air flow, and b) pointed downstream. The color bar is proportional to backscatter intensity and is in units of ***probability of detection per pixel per meter per laser pulse.***

One of the goals of this campaign was to measure the aerosol detection sensitivity of the photon-counting ladar sensor. The ECBC Vortex Chamber is nearly ideal as it provides a controlled volume and releases of known type and quantity. In order to estimate the ladar sensor's sensitivity, we ran the chamber for 30 minutes to evacuate aerosols from the previous release, then we released a relatively small quantity, 18 mg, of AZRD (0-5 micron particle sizes), and compared the ladar data (integrated over volume and time) to that of the APS particle counter (single point location). In this case, the background-subtracted ladar data were integrated within the entire volume of the sensor's field of view and over 5-second intervals (67,500 laser pulses). Figure 9 shows an over-plot of the resulting average ladar particle density and APS measured particle density versus relative time. Both plots show a rapid rise shortly after the corresponding aerosol release. The two sensors did not share a common time base, so the two plots were aligned in time using this rapid rise. The APS was reporting a background concentration of ~ 1 particle per cc, or 1000 particles per liter (PPL) just before this release.

The ladar sensitivity estimate is derived from the data shown in figure 9 and using the APS particle counter as "Ground Truth". At the peak of this plot, the APS (shown as a continuous red line) reports a particle density (at one location) of roughly 50-kppl, or equivalent 50,000 Agent Containing Particles per Liter of Air (ACPLA). We estimate that the integrated ladar data (black dots) shows a Signal to Noise Ratio (SNR) of approximately 5 or 6. Therefore, we define the ladar sensitivity (under the conditions of this test) in terms of its Noise Equivalent ACPLA of roughly 10,000.

$$NEACPLA_{LadarSensitivityLimit} \sim 10k$$

This value is approximately equal to the ambient air density (at the time of these tests) outside chamber and inside the chamber before it was operated to clean the air within (as shown in Figure 3).

Figure 9 also shows an obvious divergence of these two plots about one minute after the release. There are a number of possible explanations for this discrepancy, but the team has not determined its cause.

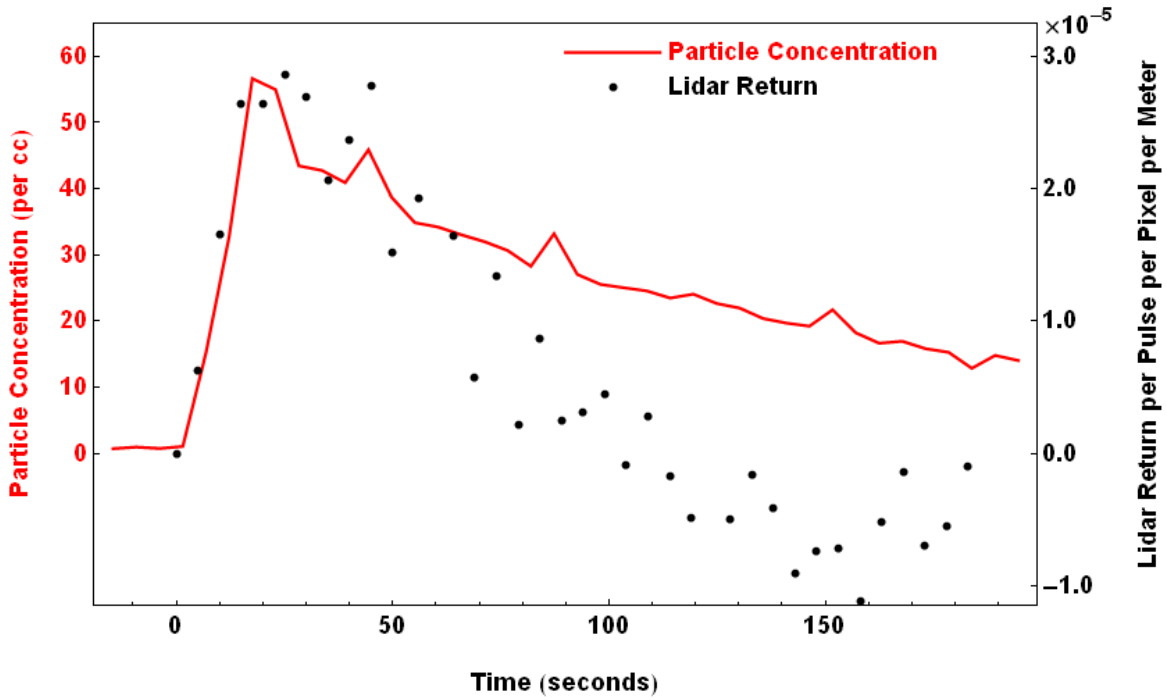

Figure 9: Two plots of the observed particle density versus time after a release of 18 mg AZRD (0-5 micron particle size). Data from the APS particle counter (single location) is shown as a continuous red line' the ladar data (averaged over entire FOV volume) is shown as black dots.

4. FUTURE NEEDS

There are many commercial and defense applications for remote sensing of aerosols, such as, for emissions monitoring or detection of biological agents. Furthermore, any effective and rapid defensive response to a biological attack will require low-latency answers to the following questions:

1) What is it (and specifically how harmful)?
2) Where is it (and where did it originate)?
3) Where is it going (possibly to trigger protective action)?

Active imaging remote sensors, such as ladar, are maturing rapidly, and can provide an enabling capability to monitor extended volumes of air above and around locations requiring protection. The photon-counting ladar sensor technologies developed and demonstrated by MIT Lincoln Laboratory is a proven architecture that can reduce the required size, weight, volume, and cost of active imaging.

The MAIL sensor was designed and developed to image hard targets from a low-altitude airborne platform, yet it worked quite well to demonstrate high-resolution spatial-temporal imagery of aerosol releases. The data we've collected can be used to engineer robust sensors that are designed to satisfy operational requirements. We have demonstrated the capability to detect and track small quantities of aerosols (likewise, relatively small changes in density). However, agent specificity will require additional information.

5. SUMMARY

A "quick and dirty" field test was conducted to achieve two goals: 1) to measure the spatial and temporally resolved distribution of aerosols released within the Edgewood Chemical and Biological Center (ECBC) Vortex Chamber, and, 2) estimate the sensitivity of one of the photon-counting ladar sensors developed by MIT Lincoln Laboratory. The Mobile Active Imaging Ladar (MAIL) has identical sensor parameters as that system known as Jigsaw Phase 2, and was operated with the ladar field of view passing through the open windows of the Vortex Chamber and the building housing the chamber. Samples of Arizona Road Dust, of known particle size ranges, was used in a series of release tests.. 3-D ladar data were recorded along with a single "ground truth" particle counter (positioned inside the chamber). The processed ladar data provides unprecedented spatially and temporally resolved particle densities as the aerosols from a point release are distributed within, and eventually removed from, the Vortex Chamber.

The controlled releases and environment at the ECBC Vortex Chamber provided a unique opportunity to measure the aerosol detection sensitivity of the photon-counting ladar. Although the ladar was designed to image hard target surface at ranges typically greater than 150 meters, and was out of focus for theses tests (where the chamber volume was estimated by the lidar to be between 73 and 79 meters range), the sensor system worked quite well. Under the conditions of the test, we estimate the MAIL ladar noise equivalent sensitivity limit is about 10kppl. This particle density is at or near that of the ambient particle density outside the chamber during these tests.

The two main goals of this field test were successfully achieved. The data and results can be used to plan more extensive Test Range experiments, and/or derive the requirements for operational ladar sensors.

6. ACKNOWLEDGEMENTS

This work would not have been possible without the assistance and support from several people from the US Army's Edgewood Chemical and Biological Center (ECBC). We wish to acknowledge the technical and management support provided by Francis M. D'Amico, Joseph R. Mashinski, and Raphael P. Moon. Also, operations and support at the ECBC Vortex Chamber were expertly provided by Robert Knapp and Bob Doherty.

REFERENCES

[1] Marino, R., M., Davis Jr., W. R., "Jigsaw: A Foliage-Penetrating 3D Imaging Laser Radar System," Lincoln Laboratory Journal 15(1), (2005).

[2] Marino, R. M., Stephens, T., Hatch, R. E., McLaughlin, J. L., Rowe, G. S., Mooney, J. G., O'Brien, M. E., Adams, J. S., Skelly, L., Knowlton, R. C., Forman, S. E., Davis Jr., W. E., "A compact 3D imaging laser radar system using Geiger-mode APD arrays: system and measurements," Proc. SPIE 5086, (2003).

[3] Albota, M.A., Aull, B.F., Fouche, D.G., Kocher, D.G., Heinrichs, R.M., Marino, R.M., Zayhowski, J.J., Player, B.E., Willard, B.C., Mooney, J., O'Brien, M., and Carlson, R.R., "Three-Dimensional Imaging Laser Radar Using Geiger-mode Avalanche Photodiode Arrays and Short-pulse Microchip Lasers," Lincoln Laboratory Journal 13(2), (2002).

[4] Aull, B. F., Loomis, A. H., Young, D. J., Heinrichs, R. M., Felton, B. J., Daniels, P. J., and Landers, D. J., "Geiger-Mode Avalanche Photodiodes for Three-Dimensional Imaging," Lincoln Laboratory Journal 13(2), (2002).

[5] Heinrichs, R.M. Aull, B.F., Marino, R.M., Fouche, D.G., McIntosh, A.K., Zayhowski, J.J., Stephens, T., O'Brien, M.E., Albota, M. A., "Three-Dimensional Laser Radar with APD Arrays," Proc. SPIE Laser Radar Technology and Applications VI 4377, (2001).

[6] Marino, R. M., Bohrer, M. J., "A Photon-Counting 3-D Imaging Laser Radar," Proc. Lasers '94, (1994).

[7] Marino, R. M., Spitzberg, R. M., Bohrer, M. J., "A Photon Counting 3-D Imaging Laser Radar for Advanced Discriminating Interceptors," Proc. 2nd Annual AIAA SDIO Interceptor Technology Conference 2644, (1993).